QUANTITATIVE DETERMINATION OF HYDROQUINONE VIA ELECTROCHEMICAL METHODS AT A NANO-ARCHITECTURE PLATINUM ELECTRODE

Ahmed A. Al-Owais[1], Ibrahim S. El-Hallag[2*], Elsayed H. El-Mossalamy[3]

[1]*Chemistry Department, College of Science, King Saud University, Riyadh, Saudi Arabia*
[2]*Chemistry Department, Faculty of Science, Tanta University, Tanta, Egypt*
[3]*Chemistry Department, Faculty of Science, Benha University, Benha, Egypt*
i.elhallag@yahoo.com

Hydroquinone (HQ) was electrochemically measured using convolutive cyclic voltammetry and differential pulse voltammetry (DPV) on a nano-architecture mesoporous platinum film electrochemically grown from a hexagonal liquid crystalline template of C16EO8 surfactant in 1.0 mol/l $HClO_4$. The HQ cyclic voltammograms produced one oxidative peak in the forward sweep of potential and one reductive peak in the reverse sweep. The effect of HQ concentration was investigated using the different electro-chemical methods mentioned above. The modified platinum electrode exhibits good sensitivity for the determination of the HQ compound in 1.0 mol/l $HClO_4$. The best executive was found for the i-t curve method developed from cyclic voltammetry of HQ. It exhibits a linear peak current response over the concentration range of 8 to 55 μmol/l, with a detection limit of 0.5726 μmol/l and a quantification limit of 1.9088 μmol/l, confirming the accuracy and sensitivity of this quick, cheap, and easy method.

Keywords: hydroquinone; convolutive cyclic voltammetry; mesoporous; hexagonal; platinum

КВАНТИТАТИВНО ОПРЕДЕЛУВАЊЕ НА ХИДРОХИНОН СО УПОТРЕБА НА ЕЛЕКТРОХЕМИСКИ МЕТОДИ НА НАНО-АРХИТЕКТУРНА ПЛАТИНСКА ЕЛЕКТРОДА

Електрохемискиот одговор на хидрохинон (HQ) беше детектиран со помош на конволутивна циклична волтаметрија и диференцијална пулсна волтаметрија (DPV) на нано-архитектурен мезопорен филм од платина, кој беше електрохемиски синтетизиран од хексагонална течно-кристална форма на сурфактантот C16EO8 во силно кисел медиум од перхлорна киселина со концентрација 1 mol/l. Во цикличните волтаграми на HQ беше регистриран еден добро дефиниран пик во оксидациска насока и еден редукциски пик во обратен потенцијален циклус на промена на потенцијалот. Влијанието на концентрацијата на HQ врз волтаметриските одговори беше испитано со користење на погоре наведените електрохемиски техники. Модифицираната платинска електрода покажа добра осетливост во однос на квантитативното определување на соединението HQ во перхлорна киселина со концентрација од 1 mol/l. Најдобри резултати од аналитичка гледна точка беа добиени со методот на *i-t* крива кој беше развиен од цикличните волтаграми на HQ. Овој конволуциски волтаметриски метод покажа линеарен одговор на струјата на пикот во концентрациски опсег на HQ од 8 μmol/l до 55 μmol/l, со граница на детекција од 0.5726 μmol/l и граница на квантификација од 1.9088 μmol/l. Овие податоци служат како релевантни индикатори на точноста и осетливоста на овој брз, евтин и лесен волтаметриски метод.

Клучни зборови: хидрохинон; конволутивна циклична волтаметрија; хексагонална платина.

1. INTRODUCTION

Dihydroxybenzenes are important phenolic compounds with high toxicity and low degradability. They are suspected of being carcinogens and are widely released into the environment since they are used as chemical intermediates for synthesizing a variety of pharmaceuticals and other organic compounds such as dyes, photography chemicals, plastics, flavoring agents, antioxidants, rubber, and pesticides. Therefore, they have been listed as priority pollutants by environmental organizations such as the US-EPA and the EU.[1,2] Hydroquinone (HQ, 1,4-dihydroxybenzene) is a pharmaceutical product extensively used for the treatment of skin diseases. As a skin-whitening product, HQ inhibits the enzymatic pathway of tyrosinase, preventing it from producing the pigment melanin from dopamine.[3,4] Due to the extraordinary toxicity of HQ at high concentrations, it causes nausea, edema of internal organs, headaches, dizziness, and even kidney damage in humans.[5] Numerous analytical procedures have been employed to quantify HQ, including chromatography,[6] fluorescence,[7] spectrophotometry,[8] fluorometry,[3] and electrochemical methods.[3,5] Most of the mentioned instrumental methods are time-consuming and costly and require complicated sample preparation procedures and an expert operator, making them unsuitable for routine analysis. In contrast, electrochemical techniques have received extraordinary attention due to their low cost, rapid response, ease of operation, low detection limit, and relatively short analysis time.[9,10] Coenzyme Q10 (CoQ10) is one of the essential components of the mitochondrial electron-transport chain (ETC) with the primary function of transferring electrons along and protons across the inner mitochondrial membrane (IMM). It is able to bind and transport Ca^{2+} across artificial biomimetic membranes.[11] Cyclic voltammetry studies are reported for two representative quinones, benzoquinone and 2-anthraquinonesulfonate, in buffered and unbuffered aqueous solutions at different pH's.[12] Quinones constitute a big family of organic redox-active compounds that are overwhelmingly involved in important physiological processes. The most important members in the class of quinones are the plastoquinones and coenzyme Q (CoQ) derivatives. Voltammetry of coenzyme Q family members has attracted significant attention since 50 years ago.[13] Protein-film voltammetry (PFV) is considered the simplest methodology to study the electrochemistry of lipophilic redox enzymes in an aqueous environment. The PFV methodology enables access to the relevant thermodynamic and ki-

netic parameters of the enzyme electrode reaction and enzyme-substrate interactions, which are important to better understand many metabolic pathways in living systems and to delineate the physiological role of enzymes.[14] Recent advances in square-wave voltammetry for analytical purposes as well as for studying electrode mechanisms and kinetics are reviewed, mainly covering results published in the last decade.[15] Voltammetry has made a huge impact in many different scientific fields such as physics, chemistry, pharmacy, medicine, biofuel cells, and environmental protection.[16] Recently, a few modified electrochemical sensors were developed for the determination of HQ in biological and pharmaceutical samples.[3–5] Among the modified electrodes, the nano-architecture electrode has received extraordinary attention due to its advantages of easy preparation, generous surface chemistry, stable response, wide potential window, and low ohmic resistance. In addition to all the benefits mentioned, the use of modifiers that effectively accelerate and facilitate electron transport between the analyte and the electrode has made the nano-architecture electrodes suitable candidates for the measurement of the analytes by reducing the overpotential required for the electrode reactions.[17,18] The unique physicochemical characteristics of the mentioned materials have resulted in a better electrochemical response of the modified Pt electrode, particularly for the quantitative determination of trace analytes.[19,20] Pt powder in a pluronic, lyotropic, liquid crystal template (LLC) with remarkable chemical and thermal stability, acceptable electrochemical windows, and desirable conductivity properties has received considerable attention in modifying the ordinary Pt electrode. The LLC provides benefits such as improving the electron transfer rate, sensitivity, and conductivity of the nano-architecture Pt electrode compared to a bare Pt electrode.[21] The metal nanoparticles provide a larger active surface area with desired catalytic activity for facilitating the electron transport between the analyte and Pt electrode surface, and Pt metal nanoparticles have been extensively applied in the fabrication of electrochemical sensors.[22,23] Moreover, metal nanoparticles, as efficient catalysts, enhance the electrochemical reactions of electrochemical sensors.[6,24–26] Recently, the design and construction of electrochemical sensors have attracted more interest in the field of analytical and bioanalytical electrochemistry. The developed sensors are normally based on the structure of a working electrode.[27,28] It is well known that conventional plain electrodes display poor selectivity and sensitivity along with fouling of sig-

nals in the detection of HQ.[29,30] Modification of the conventional working electrodes is a smart method to construct HQ sensors having high selectivity, low oxidation potential, and high sensitivity. One of the most promising methods to modify the electrode is the electrochemical deposition of nano-architecture mesoporous metal films. These mesoporous metal films can be obtained with the aid of a template formed by hexagonal, lyotropic, liquid crystalline substances.[31–33] The mesoporous metal layers have a very high surface area (roughness) due to the presence of a highly arranged hexagonal array of cylindrical nanopores. Electrodeposition conditions and template mixtures represent the key parameters for determining pore radius and separation distance, which are usually in the range of 1–10 nm. The nano-architecture mesoporous Pt layer has attracted much attention because of its uses in electrocatalysis.[34–36] Therefore, great attempts have been made to develop a highly sensitive sensor for the quantitative determination of trace amounts of HQ using the proposed nano-architecture Pt electrode. To the best of our knowledge, this is the first time a convolution, deconvolution voltammetry method has been developed for the determination of HQ.

2. EXPERIMENTAL

2.1. *Reagents*

The chemicals obtained were analytical grade and used without further purification. $HClO_4$ and hydroquinone (HQ) were purchased from Aldrich. Deionized and filtered water were taken from an Elga water purification system.

2.2. *Instrumentation*

Electrochemical experiments were carried out in a conventional three-electrode cell using a Micro-Autolab Type III system (Eco Chemie, NL). A saturated calomel electrode (SCE) was used as the reference electrode, and about 1 cm^2 of platinum gauze as the counter electrode. The working electrode was a 1 mm diameter Pt disc with a surface area of $7.85 \cdot 10^{-3}$ cm^2. All the electrochemical experiments were performed at room temperature (23 ± 2 °C).

2.3. *Preparation of the nano-architecture platinum film*

A hexagonal liquid crystalline plating template mixture was prepared using the method established in the literature by dissolving hexachlo-

roplatinic acid (HCPA) (20 wt%) in distilled water (40 wt%).[37] The resulting solution was mixed with melted $C_{16}EO_8$ surfactant (40 wt%) at 45 °C. Prior to the electrodeposition of the mesoporous Pt film, the working polycrystalline Pt disc electrode with a 1 mm diameter was polished using 1 µm alumina and washed with water, followed by electrochemical cleaning by sweeping in 2 mol/l H_2SO_4 in a potential range from +0.25 to +1.4 V *vs*. SCE for 20 cycles at a scan rate of 100 mV s^{-1}. The mesoporous nano-architecture platinum films were electrochemically deposited from the template mixture at a constant potential of 100 mV *vs*. SCE. After electrodeposition, the template mixture was removed from the mesoporous Pt films by soaking overnight in agitated water at 40 °C. This cleaning process was also performed before each experiment and afterward.

3. RESULTS AND DISCUSSION

3.1. *Cyclic voltammetry behavior of the HQ Pt electrode in nano-architecture*

In order to study the electrochemical behavior of the HQ in acidic media, cyclic voltammograms were recorded at a nano-architecture Pt electrode for 8 µmol/l hydroquinone in a 1.0 mol/l $HClO_4$ solution at a scan rate of 50 mV s^{-1}. As shown in Figure 1, the anodic and cathodic peak potentials are located at 468 and 397 mV *vs*. SCE, respectively. The peak-to-peak separation, ΔE_p, of HQ was found to be 71 mV, which clearly indicates that HQ oxidation possesses moderately fast charge transfer kinetics at the nano-architecture Pt electrode.
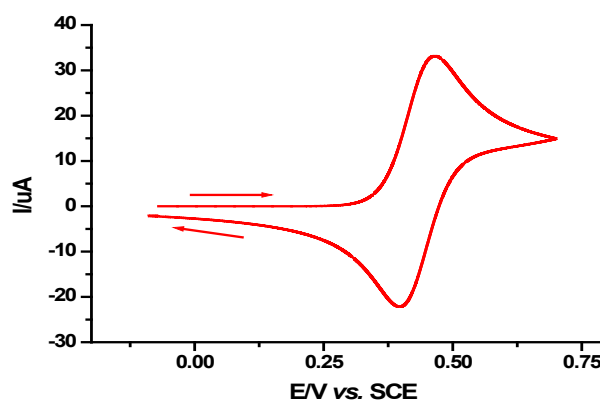
Fig. 1. Cyclic voltammetry at a scan rate of 50 mV s^{-1} for 8 µmol/l HQ in 1.0 mol/l $HClO_4$ at the nano-architecture Pt electrode

Figure 2 shows a set of representative cyclic voltammograms for HQ at the nano-architecture platinum electrode in 1.0 mol/l $HClO_4$ containing

different concentrations of catechol (8–55 μmol/l). The ratio of the cathodic peak current to the anodic peak current, i_{pc}/i_{pa}, is about 0.95, which is very close to unity, indicating the stability of the 1,2-benzoquinone oxidation product in the solution.
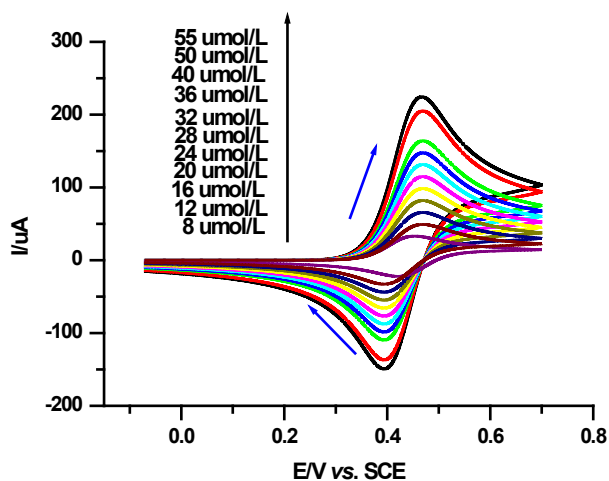
Fig. 2. Cyclic voltammetry of HQ at different concentrations, scan rate 50 mV s^{-1} in 1.0 mol/l HClO$_4$ at a nano-architecture Pt electrode

Figure 2 displays the effect of increasing the HQ concentration from 8 μmol/l to 55 μmol/l on the corresponding CV recorded at the nano-architecture Pt electrode in 1.0 mol/l HClO$_4$ with a scan rate of 50 mV s^{-1}. It was observed that the anodic and cathodic peak currents increase with the increase in HQ concentration, and the peak-to-peak separation, ΔEp, increases slightly. For characterization of the electrochemical method, the limit of detection (LOD), correlation coefficient (R^2), and limit of quantification (LOQ) were calculated using eleven data points according to the Miller and Miller method.[38] The calibration curve of HQ at different concentrations is represented in Figure 3. As indicated by Figure 3, the anodic peak

current response, i_{pa}, (peak height), and the concentrations of analyte (HQ) are linearly dependent within the 8–55 μmol/l concentration, following the linear regression Eqs. 1 and 2:[39]

$$y = mx + z \quad (1)$$

where m is the slope of the regression line, and z is the point at which the line crosses the y-axis (y-intercept). In our case, the y-axis represents the anodic peak current ($I_{p,a}/\mu A$), and the x-axis is the analyte concentration c (HQ)/μmol l^{-1}. From Figure 3, we obtain the following equation:

$$\frac{ipa}{\mu a} = \frac{ipa}{\mu A} \quad (2)$$

The standard deviation (SD/μA) of the linear regression for the anodic peak current vs. analyte concentrations, shown in Figure 3, is 2.101. Consequently, the calculated SD/μA value was then used to determine the limits of detection (LOD) and quantification (LOQ) values using the following Eq.3.[40]

$$LOD \text{ or } LOQ = F \frac{SD}{m} \quad (3)$$

where m is the slope, SD/μA is the standard deviation, and F is the factor 3 or 10 for LOD and LOQ, respectively. To conclude, according to Eq. 2 and Figure 3, the value of R^2 is 0.9995, which shows excellent linear fitting within the studied concentration range. Moreover, the nano-architecture Pt electrode exhibits good LOD and LOQ for HQ, with values of 1.53 and 5.102 μmol/l, respectively.

A comparison of the nano-architecture Pt electrode with other modified working electrodes for the magnitude of the LOD (μmol/l) established in the literature is summarized in Table 1.[39–49]
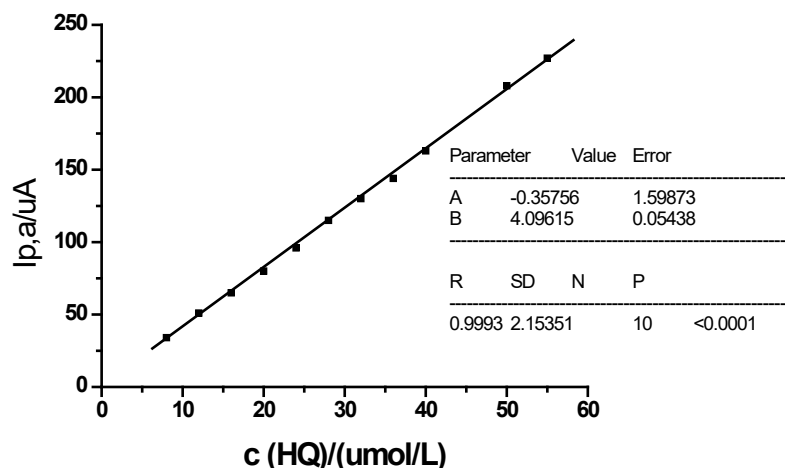
Fig. 3. Plot of $I_{p,a}$ /μA versus c (HQ)/μmol/l built from Fig. 2

T a b l e 1

Comparison between the mesoporous Pt electrode and other modified working electrodes used for HQ quantification

Working electrode	LOD(µM)	LOQ(µM)	Method	Ref.
PNR/MCPE[a]	6.40	---	CV	[39]
RGO-MWCNTs/GC[b]	1.80	---	CV	[40]
Poly(calmagite) MCPE[c]	1.75	---	CV	[41]
Poly(BGA)/MCPE[d]	2.55	---	CV	[42]
Poly(oPD)/MCPE[e]	1.10	---	CV	[45]
P4NA/MGCE[f]	3.90	---	DPV	[49]
Mesoporous Pt	1.53	5.10	CV	This work
Mesoporous Pt	0.57	1.90	Conv.	This work
Mesoporous Pt	1.55	5.18	Decon.	This work
Mesoporous Pt	1.49	4.99	*i*-t curve	This work
Mesoporous Pt	1.69	5.66	DPV	This work

[a]Carbon paste electrode modified with poly (neutral red), [b]Glassy carbon electrode modified with carbon nanotubes and reduced graphene oxide, [c] Carbon paste electrode modified with poly (calmagite), [d]Carbon paste electrode modified with poly (butyl glycol acetate), [e]Carbon paste electrode modified with *o*-phenylenediamine, [f] Glassy carbon electrode modified with poly(4-nitroaniline)

3.2. *Convolution voltammetric analysis of HQ at a nano-architecture Pt electrode*

Convolution voltammetry is a mathematical procedure used in electrochemistry to analyze the response of an electrode to a perturbation of its potential. It involves convolving the current response with a function that describes the perturbation, which allows for the elimination of the effect of the decrease of the concentration gradient from the total response of the electrode.[46] The method is concerned with quantities that are directly related to the concentration of electroactive species at the electrode surface. Convolution voltammetry uses the convolution principle to convert cyclic voltammograms into steady-state curves.[46,47] The current reaches its limiting value, which is independent of the excitation signal, in cases of diffusion-controlled mass transfer of active species. The convoluted current $I_l(t)$ should theoretically reach a limiting value I_{lim}, as indicated by the presence of a flat plateau in the data, as described by Eq. 4:

$$I_{lim} = nFAcD^{0.5},\qquad(4)$$

where *n* is the number of transferred electrons, *F* is Faraday's constant (96485 C mol^{-1}), *A* is the surface area of the electrode, *D* is the diffusion coefficient of the electroactive species, and *c* is the bulk concentration of the electroactive species.

As shown in Eq. 4 and Figure 4, the resulting plateau (I_{lim}) is flat and independent of the scan rate used. So, the observed transformation of the current remains constant, leading to the accuracy of the I_{lim} determination.

The scale on the *y*-axis represents *Cs(t)* nFAD$^{1/2}$, where *Cs(t)* is the concentration of the product of the electron transfer step on the electrode's surface. The effect of increasing the concentration of HQ in the range of 8–55 umol/l on the corresponding convolution voltammetry recorded at a nano-architecture Pt electrode in 1.0 mol/l HClO$_4$ with a scan rate of 50 mV s^{-1} is shown in Figure 4. The anodic limiting current (I_{lim}) increases as the concentration of HQ increases. Convolution voltammetry was used to determine the limit of detection (LOD), determination coefficient (R^2), and limit of quantification (LOQ) of HQ.[38]
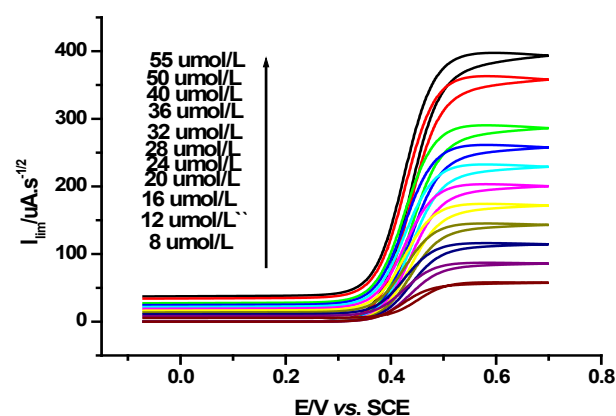
Fig. 4. Convolution voltammetry of HQ at different concentrations, scan rate 50 mV s^{-1} in 1.0 mol/l HClO$_4$ at a nano-architecture Pt electrode

Figure 5 depicts the calibration curve for HQ at various concentrations. As indicated in Figure 5, the anodic limiting current response (I_{lim} height) and the analyte (HQ) concentrations are linearly

dependent within the 8–55 μmol/l concentration range, following the linear regression equations 1 and 4.[39] In this case, the y-axis represents the anodic limiting current (I_{lim}, μA. $S^{-1/2}$) and the x-axis the analyte concentrations (c, μmol/l). Then from Figure 5, we get the following:

$$\frac{I_{lim}}{\mu As^{-1/2}} = 7.13\, c\left(\frac{\mu mol}{L}\right) + 0.904 \qquad (5)$$

Herein, the SD/μA of the linear regression for the anodic limiting current vs. analyte concentrations stated in Fig. 5 equals 1.36118. Consequently, the calculated SD/μA value was then used to determine the limits of detection (LOD) and quantification (LOQ) values according to Eq. 3.[40] Based on Eq. 5 and Figure 5, the value of R^2 is 0.99993, which shows excellent linear fitting within the studied concentration range. Moreover, the mesoporous Pt electrode exhibits good LOD and LOQ for HQ, with values of 0.5726 and 1.908 μmol/l, respectively.

| A | 0.90406 | 0.9241 |
| B | 7.13101 | 0.02837 |

| R | SD | N | P |
| 0.99993 | 1.36118 | 11 | <0.0001 |
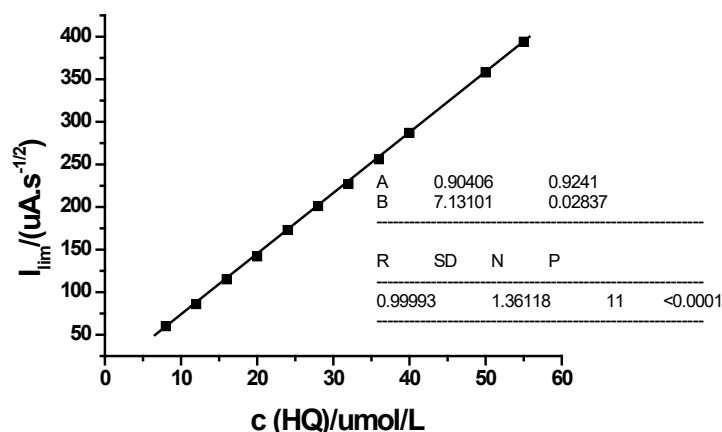
Fig. 5. Graph of I_{lim} / μA $s^{-1/2}$ versus c(HQ)/μmol/l built from Figure 4

3.3. Deconvolution voltammetric analysis of HQ at a nano-architecture Pt electrode

The principle of deconvolution voltammetry is that a mathematical data processing procedure is used in electrochemistry to separate overlapping signals from different electrochemical reactions. It involves fitting whole voltammetric curves to separate the signals, which is most effective for bell-shaped voltammetric signals. The approach can be applied to enhance the detection of signals that are delayed and smeared, such as in the case of ring signals. It is also used to measure the kinetics of adsorption-controlled reactions at carbon electrodes.[48] Deconvolution voltammetry actually suggests a range of tricks that may improve voltammetric measurements. It has the advantages of high sensitivity and accuracy for the determination of species and provides a better baseline for the HQ analysis. The deconvolution of the current (dI_1/dt) as a function of the potential of a reversible process is defined as follows: [48]

$$ep = \left(\frac{dI_1}{dt}\right) = \frac{nFAc\sqrt{D}a\zeta}{(1+\zeta)^2} \qquad (6)$$

where ep is the height of the deconvolution peak, a = nvF/RT, and $\zeta = \exp[n$F/R$T(E - E^0)]$, n is the

number of transferred electrons, F is Faraday's constant (96485 C mol⁻¹), ν is the scan rate in mV s⁻¹, A is the surface area of the electrode, D is the diffusion coefficient of the electroactive species, c is the bulk concentration of the electroactive species, R is the universal gas constant, T is the absolute temperature, E is the electrode potential, and E⁰ is the standard electrode potential.

It was established that Eq. 6 had been derived for the height of deconvolution peak current $ep = (dI1/dt)$, and it corresponds to a reversible reaction (Eq. 7).[46–48]

$$ep = \left(\frac{dI_1}{dt}\right) = 0.2972\, Av\frac{n^2F^2c\sqrt{D}}{RT} \qquad (7)$$

According to Eqs. 6 and 7 and Figure 6, the resulting deconvolution voltammogram is peak-like (ep) and dependent on the electroactive substance concentration and scan rate. This means that as HQ concentration and scan rate increase, the current of deconvolution voltammetry increases, reflecting the accuracy in determining the deconvolution peak height (ep). The presentation of (dI_1/dt) vs. the potential of HQ is indicated in Figure 6, and the peak height of deconvolution (ep) is described on the y-axis, while the potential is described on the x-axis.
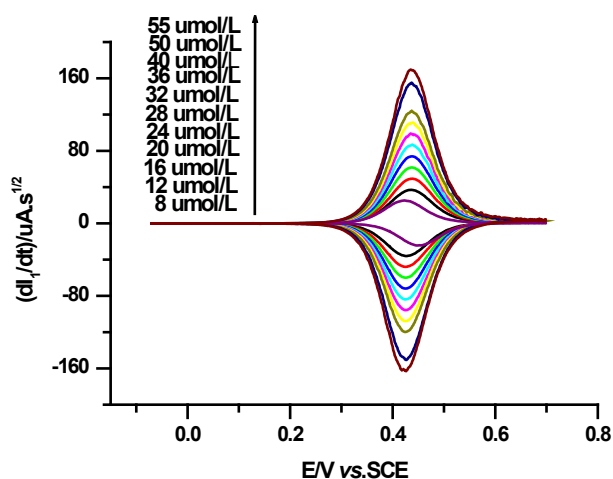
Fig. 6. Deconvolution voltammetry of HQ at different c(HQ)/μmol l^{-1}, scan rate 50 mV s^{-1} in 1.0 mol/l HClO$_4$ at a nano-architecture Pt electrode

Figure 7 shows the increasing concentration of HQ in the range of 3–55 μmol/l at the nano-architecture Pt electrode in 1.0 mol/l HClO$_4$ at a scan rate of 50 mV s^{-1}. It was noted that the deconvolution peak height current (ep) increases with increasing HQ concentration. Here, the limit of detection (LOD), determination coefficient (R^2), and limit of quantification (LOQ) of HQ were calculated via deconvolution.

Herein, the standard deviation (SD/μA) of the linear regression for the anodic deconvolution peak height *vs.* analyte concentrations stated in Figure 7 equals 1.588. Consequently, the calculated SD/μA value was then used to determine the limits of detection (LOD) and quantification (LOQ) values according to Eq. 3.[40,34] Based on Eq. 8 and Figure 7, the value of R^2 is 0.9994, which shows the existence of a positive correlation within the studied concentration range. Moreover, the nano-architecture Pt electrode exhibited good LOD and LOQ for HQ, with values of 1.555 and 5.185 μmol/l, respectively.

Fig. 7. Graph of ep versus c(HQ)/μmoll^{-1}, built from Figure 6

3.4. *Current-time curves built from CV for analysis of HQ at a nano-architecture Pt electrode*

The current-time curve arises from converting the cyclic voltammogram (*i-E* curve) into the current-time curve, and this conversion allows measuring the height of peak current in a simple and more accurate manner. Figure 8 displays the *i-t* plot of HQ in the range of 8–55 μmol/l at a nano-architecture Pt electrode in 1.0 mol/l HClO$_4$ with a scan rate of 50 mV s^{-1}. It

was noted that the anodic and cathodic peak currents of the *i-t* curve increase with increasing concentrations of HQ. The limits of detection (LOD), determination coefficient (R^2), and limit of quantification (LOQ) were calculated using eleven data points as established by the Miller and Miller method.[32] The *i-t* curves of HQ at different concentrations are displayed in Figure 8. As shown in Figure 9, the forward anodic peak currents of the *i-t* plot (peak height) versus the analyte (HQ) concentrations are linearly depend-

ent within the concentration range of 8–55 μmol/l, following the linear regression equations (1) and (2). From Figure 9, we found the following:

$$Ip(\mu A) = 4.128\, c\left(\frac{\mu mol}{L}\right) + 1.399 \qquad (8)$$

Herein, the SD/μA of the linear regression for the anodic peak current *vs.* analyte concentrations stated in Figure 9 equals 2. Consequent-

ly, the calculated SD/μA value was then used to determine the limits of detection (LOD) and quantification (LOQ) values, as indicated in Eq. 3.[40] The value of R^2 is 0.99951, which shows excellent linear fitting within the studied concentration range. Moreover, the nano-architecture Pt electrode exhibited good LOD and LOQ for HQ, with values of 1.4977 and 4.992 μmol/l, respectively.
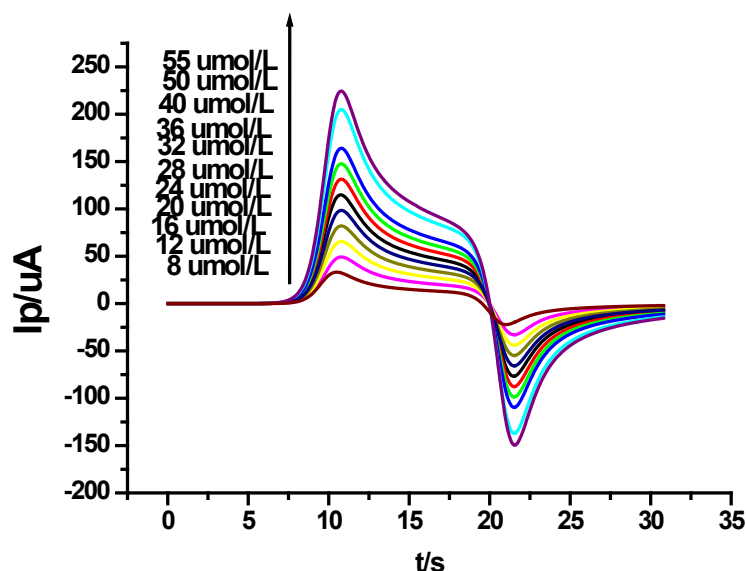
Fig. 8. Current-time curves built from the CV of HQ at different concentrations were recorded at a scan rate of 50 mV s^{-1} in 1.0 mol/l HClO$_4$ at a nano-architecture Pt electrode
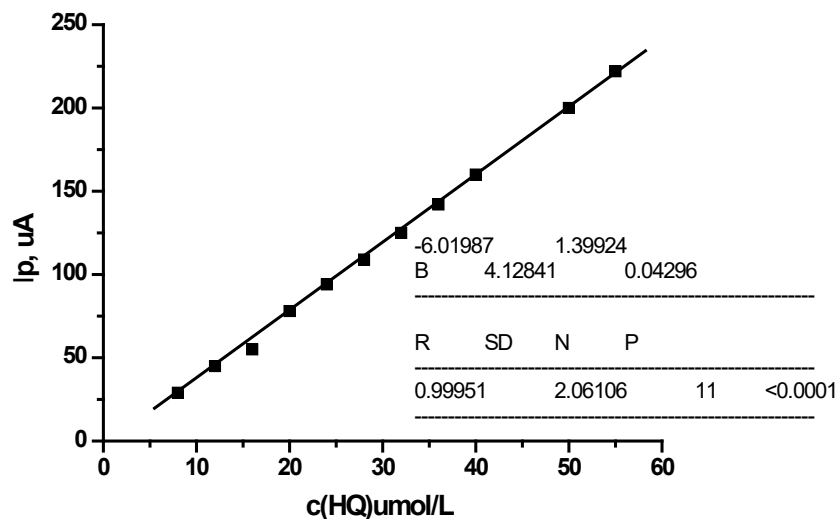
Fig. 9. Current versus different concentrations of HQ, built from Figure 8

3.5. *Differential pulse voltammetry study of HQ at a nano-architecture Pt electrode*

Differential pulse voltammetry was used to investigate the sensitivity of a nano-structured Pt

electrode for the detection and quantification of HQ (DPV). The DPV experiments were recorded at the optimum conditions: 10 mV s^{-1} scan rate, 50 ms pulse width, and 30 mV pulse amplitude. Figure 10 shows the DP voltammograms for 5 μmol/l

HQ in 1.0 mol/l $HClO_4$ at mesoporous Pt electrodes. It is obvious that the height of the oxidative peak increases with increasing the concentration of HQ at the mesoporous Pt electrode. Figure 10 clarifies the dependence of the DPV peak current on the concentration of HQ.
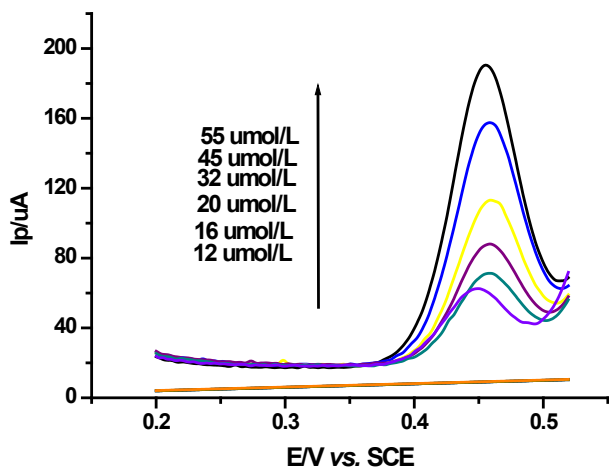
Fig. 10. Differential pulse voltammograms of HQ at different concentrations in the range from 12 to 55 µmol/l at a nano-architecture platinum electrode in 1.0 mol/l $HClO_4$

Clearly, we can see that the HQ peak current increases linearly with the concentration, in the range of 12–55 µmol/l. The detection limit (LOD), determination coefficient (R^2), sensitivity, and repeatability (RSD%) of HQ were determined via DPV.[38] As indicated in Figure 11, the peak height (i_p) of the DPV and the analyte (HQ) concentrations are linearly dependent within the 12–55 µmol/l concentration range, following the linear regression Equations 1 and 4.[39] In this case, the y-axis represents the height of the peak current (i_p, µA), and the x-axis is the analyte concentrations (c, µmol/l), from Figure 11, we obtained the following:

$$Ip(\mu A) = 17.872\, c \left(\frac{\mu mol}{L}\right) + 17.677 \quad (9)$$

The standard deviation of the linear regression for the anodic peak height of the DP voltammogram *vs.* analyte concentrations is 10.11638, as shown in Figure 11. Consequently, according to Eq. 3[40] and the SD/µA value, the detection limit (LOD) and quantification limit (LOQ) were determined. Based on Eq. 9 and Figure 11, the value of R^2 is 0.9841, which shows excellent linear fitting within the studied concentration range. Moreover, the nano-architecture Pt electrode exhibited good LOD and LOQ for CC, with values of 1.6981 and 5.6604 µmol/l, respectively.

The limits of detection (LOD) and quantification (LOQ) calculated in this work were compared to those determined in the literature and presented in Table 1. As shown in Table 1, the mesoporous nano-architecture Pt electrode exhibits good LOD and LOQ for HQ in 1.0 mol/l $HClO_4$.
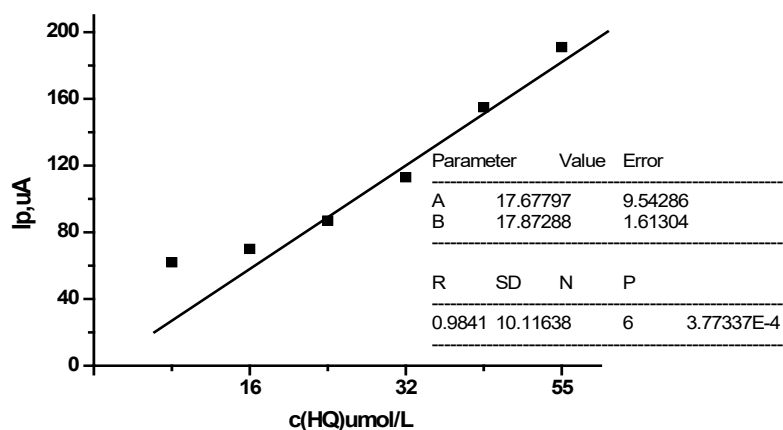
Fig. 11. Plot of dpv peak current at a nano-architecture Pt electrode *vs.* HQ concentration in 1.0 mol/l $HClO_4$

4. CONCLUSION

In this study, we established techniques for assessing the hydroquinone content of diverse substances, including pharmaceutical and cosmetic preparations, at nano-architecture platinum electrodes. The platinum electrode with a nano-architecture demonstrated high electrocatalytic activity and reversibility when it came to the oxidation of HQ. It was determined that the oxidation and reduction peak-to-peak separation (ΔE_p) is 71 mV. A wide linear range, strong repeatability, high

precision, and accuracy are also provided by the nano-architecture mesoporous platinum film electrode for a low detection limit and quantification of the HQ compound in 1.0 mol/l $HClO_4$ using a variety of contemporary electrochemical techniques. The three entirely novel, precise, and quick techniques (conv, deconv, and *i-t* curve) offer easy-to-use instruments for locating low concentrations of HQ chemicals with excellent LOD and LOQ values. The validity of the response to HQ attained in the current study also holds promise for the future effectiveness of this strategy in other analyses.

REFERENCES

(1) Hudari, F. F.; De Almeida, L. C; Da Silva, B. F.; Zanoni, M. V. B., Voltammetric sensor for simultaneous determination of p-phenylenediamine and resorcinol in permanent hair dyeing and tap water by composite carbon nanotubes/chitosan modified electrode. *Microchem. J.* **2014**, *55, 261–268.* https://doi.org/10.1016/j.microc.2014.05.007 MICROC 1955

(2) Gomez, A. R.; Olsina, R. A.; Martínez, L. D.; Silva, M. F., Simultaneous determination of cloramphenicol, salicylic acid and resorcinol by capillary zone electrophoresis and its application to pharmaceutical dosage forms. *Talanta.* **2003,** *61*, 233–238. https://doi.org/10.1016/S0039-9140(03)00267-4

(3) Yang, C.; Chai, Y.; Yuan, R.; Xu, W.; Chen, S., Gold nanoparticle–graphene nanohybrid bridged 3-amino-5-mercapto-1,2,4-triazole-functionalized multiwall carbon nanotubes for the simultaneous determination of hydroquinone, catechol, resorcinol and nitrite. *Anal.Methods.* **2013**, *5, 666–672.* https://doi.org/10.1039/C2AY26016F

(4) Zhang, H.; Bo, X.; Guo, L, Electrochemical preparation of porous graphene and its electrochemical application in the simultaneous determination of hydroquinone, catechol, and resorcinol. *Sens. Actuators B Chem.* **2015,** *220*, 919–926. DOI:10.1016/j.snb.2015.06.035

(5) Zhang, D.; Peng, Y.; Qi, H.; Gao, Q.; Zhang, C., Application of multielectrode array modified with carbon nanotubes to simultaneous amperometric determination of dihydroxybenzene isomers. *Sens. Actuators B Chem.* **2009**, *136*, 113–121. https://doi.org/10.1016/j.snb.2008.11.010

(6) Ding, Y.-P.; Liu, W.-L.; Wu, Q.-S.; Wang, X.-G., Direct simultaneous determination of dihydroxybenzene isomers at C-nanotube-modified electrodes by derivative voltammetry. *J. Electroanal. Chem.* **2005**, *575*, 275–280. https://doi.org/10.1016/j.jelechem. 2004. 09.020

(7) Pistonesi, M. F.; Di Nezio, M. S.; Centurión, M. E.; Palomeque, M. E.; Lista, A. G;. Band, B. S. F., Determination of phenol, resorcinol and hydroquinone in air samples by synchronous fluorescence using partial least-squares (PLS). *Talanta.* **2006**, *69*, 1265–1268. https://doi.org/10.1016/j.talanta.2005.12.050

(8) Prathap, M. A.; Satpati, B.; Srivastava, R., Facile preparation of polyaniline/MnO₂ nanofibers and its electrochemical application in the simultaneous determination of catechol, hydroquinone, and resorcinol. *Sens. Actuators B Chem.* **2013**, *186*, 67–77. https://doi.org/10.1016/j.snb.2013.05.076

(9) Suea-Ngam, A.; Rattanarat,P.; Chailapakul, O.; Srisa-Art, M., Electrochemical droplet-based microfluidics using chip-based carbon paste electrodes for high-throughput analysis in pharmaceutical applications. *Anal. Chim. Acta.* **2015**, *883*, 45–54. https://doi.org/10.1016/j.aca.2015.03.008

(10) Charoenkitamorn, K.; Chaiyo, S.; Chailapakul, O.; Siangproh, W., Low-cost and disposable sensors for the simultaneous determination of coenzyme Q10 and α-lipoic acid using manganese(IV) oxide-modified screen-printed graphene electrodes. *Anal. Chim. Acta*. **2018**, *1004*, 22–31. https://doi.org/10.1016/j.aca.2017.12.026

(11) Bogeski, I.; Gulaboski, R.; Kappl, R.; Mirceski. V.; Stefova, M.; Petreska, J.; Hoth, M., Calcium binding and transport by coenzyme Q. *J. Am. Chem. Soc.* **2011**, *133*, 9293–9303. https://doi.org/10.1021/ja110190t

(12) Quan, M.; Sanchez, D.; Wasylkiw, M. F.; Smith, D. F., Voltammetry of quinones in unbuffered aqueous solution: reassessing the roles of proton transfer and hydrogen bonding in the aqueous electrochemistry of quinones. *J. Am. Chem. Soc.* **2007**, *129*, 12847–12856. https://doi.org/10.1021/ja0743083

(13) Gulaboski, R.; Markovski, V.; Jihe, Z., Redox chemistry of coenzyme Q — a short overview of the voltammetric features. *J. Solid State Electrochem.* **2016**, *20*, 3229–3238. https://doi.org/10.1007/s10008-016-3230-7

(14) Gulaboski, R.; Mirceski, V., Application of voltammetry in biomedicine - recent achievements in enzymatic voltammetry. *Maced. J. Chem. Chem. Eng.* **2020**, *39*, 153–166. https://doi.org/10.20450/mjcce.2020.2152

(15) Mirceski, V.; Gulaboski, R., Recent achievements in square-wave voltammetry: a review. *Maced. J. Chem. Chem. Eng.* **2014**, *33*, 1–12. https://doi.org/10.20450/mjcce.2014.515

(16) Gulaboski, R., The future of voltammetry. *Maced. J. Chem. Chem. Eng.* **2022**, *41*, 151–162. https://doi.org/10.20450/mjcce.2022.2555

(17) Bagheri, H.; Shirzadmehr, A.; Rezaei, M.; Khoshsafar, H., Determination of tramadol in pharmaceutical products and biological samples using a new nanocomposite carbon paste sensor based on decorated nanographene/tramadol-imprinted polymer nanoparticles/ionic. liquid, *Ionics.* **2018**, *24*, 833–843. https://doi.org/10.1007/s11581-017-2252-1

(18) Zeinali, H.; Bagheri, H.; Monsef-Khoshhesab, Z.; Khoshsafar, H.; Hajian, A., Nanomolar simultaneous determination of tryptophan and melatonin by a new ionic liquid carbon paste electrode modified with SnO₂-Co₃O₄@rGO nanocomposite. *Mater. Sci. Eng. C.* **2017**, *71*, 386–394. https://doi.org/10.1016/j.msec.2016.10.020

(19) Ma, L.; Zhao, G-C., Simultaneous determination of hydroquinone, catechol and resorcinol at graphene doped

carbon ionic liquid electrode. *Int. J. Electrochem. Sci.* **2012,** *2012,* 1–9. https://doi.org/10.1155/2012/243031

(20) Yin, H.; Zhang, Q.; Zhou, Y.; Ma, Q.; Zhu, L.; Ai, S., Electrochemical behavior of catechol, resorcinol and hydroquinone at graphene–chitosan composite film modified glassy carbon electrode and their simultaneous determination in water samples. *Electrochim. Acta.* **2011,** *56,* 2748–2753. https://doi.org/10.1016/j.electacta.2010.12.060

(21) Gupta, V. K.; Jain, R.; Nayak, A.; Agarwal, S.; Shrivastava, M., Removal of the hazardous dye btartrazine by photodegradation on titanium dioxide surface. *Mater. Sci. Eng. C.* **2011,** *31,* 1062–1067. https://doi.org/10.1016/j.msec.2011.03.006.

(22) Gupta, V. K.; Ali, I.; Saleh, T. A.; Siddiqui, M.; Agarwal, S., Chromium removal from water by activated carbon developed from waste rubber tires. *Environ. Sci. Pollut. Res.* **2013,** *20,* 1261–1268. https://doi.org/10.1007/s11356-012-0950-9

(23) Yukird, J.; Kongsittikul, P.; Qin, J.; Chailapakul, O.; Rodthongkum, N., ZnO@graphene nanocomposite modified electrode for sensitive and simultaneous detection of Cd(II) and Pb(II). *Synth. Met.* **2018,** *245,* 251–259. https://doi.org/10.1016/j.synthmet.2018.09.012

(24) Daneshgar, P.; Norouzi, P.; Ganjali, M. R.; Zamani, H. A., Ultrasensitive flow-injection electrochemical method for detection of anticancer drug tamoxifen. *Talanta.* **2009,** *77,* 1075–1080. https://doi.org/10.1016/j.talanta.2008.08.027

(25) Zaheiritousi, N.; Zamani, H. A.; Abedi, M. R.; Meghdadi, S., Fabrication of a new modified Tm^3-carbon paste sensor using multi-walled carbon nanotubes (MWCNTs) and nanosilica based on 4-hydroxy salophen. *Int. J. Electrochem. Sci.* **2017,** *12,* 2647–2657. https://doi.org/10.20964/2017.04.48

(26) Boobphahom, S.; Rattanawaleedirojn, P.; Boonyongmaneerat, Y.; Rengpipat, S.; Chailapakul, O.; Rodthongkum, N., TiO₂ sol/graphene modified 3D porous Ni foam: A novel platform for enzymatic electrochemical biosensor. *J. Electroanal. Chem.* **2019,** *833,* 133–142. https://doi.org/10.1016/jelechem.2018.11.031

(27) Saglam,O.; Dilgin, D. G.; Ertek, B.; Dilgin, Y., Differential pulse voltammetric determination of eugenol at a pencil graphite electrode. *Mater Sci Eng C.* **2016,** *60,* 156–162. https://doi.org/10.1016/j. msec. 2015.11.031

(28) Naik, T. S. S. K.; Swamy, B. E. K., Poly(phenosafranine)/SAOS modified sensor for the determination of dopamine and uric acid. *Anal. Bioanal. Electrochem.* **2017,** *9,* 424–438.

(29) El-Hallag , I. S.; Ghanem, M. A.; El-Mossalamy, E. H.; Tartour, A. R., Quantitative Determination of Catechol via Cyclic Voltammetry, Convolution-Deconvolution Voltammetry, and Differential Pulse Voltammetry at a Mesoporous Nanostructured Platinum Electrode. *J. New Mater. Electrochem. Syst.* **2022,** 25, 244-250. https://doi.org/ 10.14447/ jnmes.v25i4.a04

(30) Bartlett, P. N.; Gollas, B.; Guerin, S., The preparation and characterisation of H1-e palladium films with a regular hexagonal nanostructure formed by electro-

chemical deposition from lyotropic liquid crystalline phases. *Phys.Chem.Chem.Phys.* **2002,** *4,* 3835–3842. https://doi.org/10.1039/B201845D

(31) Ghanem, M. A.; Bartlett, P. N.; Birkin, P. N.; de Groot, P.; Sawicki, M., The Electrochemical deposition of nanostructured cobalt films from lyotropic liquid crystalline media. *J. Electrochem. Soc.* **2001,** *148,* C119. https://doi.org/10.1149/1.1342178

(32) Nelson, P. A.; Elliott, J. M.; Attard, G. S.; Owen, J. R., Mesoporous nickel/nickel oxide- a nanoarchitectured electrode. *Chem.Mater.* **2002,** *14,* 524–529. https://doi.org/10.1021/cm011021a

(33) Guo, R.; Zhang, B.; Xiufeng Liu, X., Electrodeposition of nanostructured Pt films from lyotropic liquid crystalline phases on α-Al₂O₃ supported dense Pd membranes. *Appl. Surf. Sci.* **2007,** *254,* 538–543. https://doi.org/10.1016/j.apsusc.2007.06.054

(34) Birkin, P. R.; Elliot, J. M.; Watson Y. E., Electrochemical reduction of oxygen on mesoporous platinum microelectrodes. *Chem. Commun.* **2000,** 1693–1694. https://doi.org/10.1039/b004468g

(35) Evans, S. A. G.; Elliott, J. M.; Andrews, L. M.; Bartlett, P. N.; Doyle, P. J.; Denuault, G., Detection of hydrogen peroxide at mesoporous platinum microelectrodes. *Anal. Chem.* **2002,** *74,* 1322–1326. https://doi.org/10.1021/ac011052p

(36) Park, S.; Chung, T. D.; Kim, H. C., Nonenzymatic glucose detection using mesoporous platinum, *Anal. Chem.* **2003,** *75,* 3046–3049. https://doi.org/10.1021/ac0263465

(37) Kucernak, A.; Jiang, J., Mesoporous platinum as a catalyst for oxygen electroreduction and methanol electrooxidation. *Chem. Eng. J.* **2003,** *93,* 81–90. https://doi.org/10.1016/S1385-8947(02)00111-0

(38) Miller, J. N.; Miller, J. C., *Statistics and Chemometrics for Analytical Chemistry*, Pearson Education, 6th edition. Ashford Colour Press Ltd., Gosport, UK, 2010. ISBN: 0273730428, 978 -0273730422

(39) Chitravathi, S.; Swamy, B. E. K.; Mamatha, G. P.; Sherigara, B. S., Determination of salbutamol sulfate by Alcian blue modified carbon paste electrode: A cyclic voltammetric study. *Chem. Sensors.* **2013,** *3,* 1–8. https://doi.org/10.13140/RG.2.1.3522.0087

(40) Naik, T. S. S.; Swamy, B. E. K. Modification of carbon paste electrode by electrochemical polymerization of neutral red and its catalytic capability towards the simultaneous determination of catechol and hydroquinone: A voltammetric study. *J. Electroanal. Chem.***2017,** *804,* 78–86. https://doi.org/10.1016/j.jelechem.2017.08.047

(41) Umasankar, Y.; Periasamy, A. P.; Chen, S. M. Electrocatalysis and simultaneous determination of catechol and quinol by poly(malachite green) coated multiwalled carbon nanotube film. *Anal. Biochem.* **2011,** *411,* 71–79. https://doi.org/10.1016/j. ab.2010.12.002

(42) Hu, F.; Chen, S.; Wang, C.; Yuan, R.; Yuan, D.; Wang, C., Study on the application of reduced graphene oxide and multiwall carbon nanotubes hybrid materials for simultaneous determination of catechol,

hydroquinone, p-cresol and nitrite. *Anal. Chim. Acta.* **2012**, *724*, 40–46. https://doi.org/ 10.1016/j.aca.2012.02.037

(43) Ganesh, P. S,; Kuma, B. E.; Swamy, B.E.K., Electroanalysis of catechol in presence of hydroquinone at poly(calmagite) modified carbon paste electrode: A voltammetric study. *Sci. Lett. J.* **2016**, *5*, 1–8.

(44) Chetankumar, K.; Swamy, B. E. K.; Sharma, S. C., Poly(benzoguanamine) modified sensor for catechol in presence of hydroquinone: A voltammetric study. *J. Electroanal. Chem.* **2019**, *849*, 113365. https://doi.org/10.1016/j.jelechem.2019.113365

(45) Chetankumar, K.; Swamy, K., Electrochemical Investigation of catechol and hydroquinone at poly(o-phenylenediamine) modifiedcarbon paste electrode: A voltammetric study. *Anal. Bioanal. Electrochem.* **2019**, *11*, 1638–1650.

(46) A. J. Bard, L. R. Faulkner, *Electrochemical Methods: Fundamentals and Applications.* John Wiley & Sons, New York. 2nd edition, **2001**.

(47) Imbeaux, J. C.; Savéant, J. M., Convolutive potential sweep voltammetry. I: Introduction, *J. Electroanal.Chem.* **1973**, *44*, 169–187. https://doi.org/10.1016/S0022-0728(73)80244-X

(48) Lovrić , M.; Komorsky-Lovrić, S., Theory of square-wave voltammetry of two-electron reduction with the adsorption of intermediate. *Int. J. Electrochem.* **2012**, 1–8. https://doi.org/10.1155/2012/596268

(49) Hassine, C. B. A.; Kahri, H.; Barhoumi, H., Simultaneous determination of catechol and hydroquinone using nickel nanoparticles\poly-4 nitroaniline nanocomposite modified glassy carbon electrode. *IEEE. Sens. J.* **2021**, *21*, 18864–1887.